

# Profiling and Imaging Sonar Fusion based 3D Normal Distribution Transform Mapping for AUV Application

Hangil Joe, Hyeonwoo Cho, Byeongjin Kim, Juhyun Pyo, and Son-Cheol Yu

Pohang University of Science and Technology (POSTECH), Pohang, Gyeongbuk, South Korea

Email: {roboticist, lighto, kbj0607, jhpyo, sncyu}@postech.ac.kr

**Abstract**—To expand operation coverage and period of time with low cost, self-localization is needed for long range AUVs. For this, AUVs need to perceive the surrounding environment and localize its position based on the perceived information. The types of sensors that can be used for sensing environment are extremely limited in underwater because of water turbidity and low illuminance. Sonars are a conventional solution for underwater sensing, widely used for sensing underwater environment. Sonars, however, have perceptual ambiguity depending on viewpoint, and the loss of elevation information, which makes difficult to use. One of the ways to solve the difficulties of sonar is to use plenty of data acquired from varied angles and locations. More simple way is to use multiple sonars. In this study, we propose imaging and profiling sonar based 3D mapping. We presented 3D point cloud from two different sonars, and implemented NDT mapping to combine the data set. Considering the motion characteristic of AUV, we derived 4-DOF NDT algorithm and tested it in indoor water tank. As a result, we obtained consistent 3D point cloud map.

## I. INTRODUCTION

A reliable localization is a long-standing fundamental problem of AUVs. Since GPS does not work under water surface, acoustic positioning systems such as LBL, SBL, and SSDL are only feasible solution. The acoustic positioning systems, however, very expensive to install and require heavy deck support. To expand operation coverage and period of time, self-localization is needed for long range AUVs. For self-localization, AUVs need to perceive the surrounding environment and localize its position based on the perceived information. That is simultaneous localization and mapping (SLAM). Cameras and LIDARs are widely used for sensing the environment in mobile robotics on land, but, for underwater SLAM, sonars are commonly used.

Sonars are robust to water turbidity, and is a general solution for underwater sensing of AUVs. Sonars, however, have perceptual ambiguity depending on viewpoint, and the loss of elevation information, which makes difficulties not only in 3D reconstruction but also in 3D map generation using sonars. One of the ways to resolve the difficulties is 3D reconstruction by using plenty of data acquired from varied angles and locations. Data obtained from different view point can solve the ambiguity of elevation information of sonar. In this context, we used two different type of sonars; one sonar measures the horizontal projected information, and the other measures the vertical profiling information. The measurement

data from two sonars can be combined and represented using a 3D spatial representation algorithm. In this process, the lost elevation information can be reconstructed.

In this study, we implemented mapping algorithm using data obtained from two different sonars: acoustic lens-based multi-beam sonar (ALMS) and mechanically scanning profiling sonar (MSPS). The ALMS was equipped with AUV to look forward, and MSPS which rotated 90 degrees with respect to the view angle of the ALMS was mounted on the top of ALMS. For mapping of data obtained from two different sonars, we adopted Cho's point cloud generation method[1] and the Normal distribution transform (NDT)[2], and modified it for AUV application.

## II. RELATED WORK

Sonars are widely used to construct underwater map and to recognize objects on seabed. Among them, multi-beam sonars with high frequency are considered as substitution for optical system in turbid water. Many related studies have been conducted and are in progress [3][4][5][6].

Even though high frequency multi-beam sonar has sufficiently high resolution, the ambiguity of elevation information of sonar image is a Gordian knot for reconstructing 3D from sonar image. Cho et al. proposed 3D point cloud generation method using ALMS, which used the geometry of sonar beam and the motion of AUV moving forward. When AUV having ALMS passes over a rocky seabed or objects on seabed, the height of object can be estimated by calculating the distance between the limit of sonar beam and upper boundary line of highlight exceeding the limit of sonar beam (Fig. 1 and Eq. 1).

In this approach, there must be seen a slope in front of every point cloud set as shown in Fig. 3. That is because of the ambiguity that arises when an object passes through the sonars effective region that is within the vertical beam angle of the sonar. To reduce the slope and to estimate exact location of objects on seabed, a vertically scanning sonar with much small vertical angle of view (aov) is needed. For this we additionally used MSPS. The MSPS has the vertical aov of 1.8 degrees (Fig. 2) which is much smaller than that of ALMS which has the aov of 14 degrees.

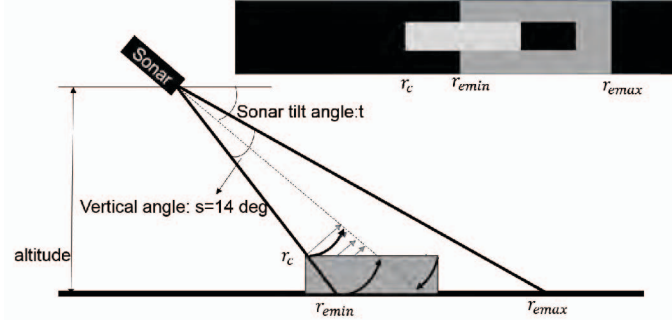


Fig. 1. Geometry of ALMS for Point cloud generation

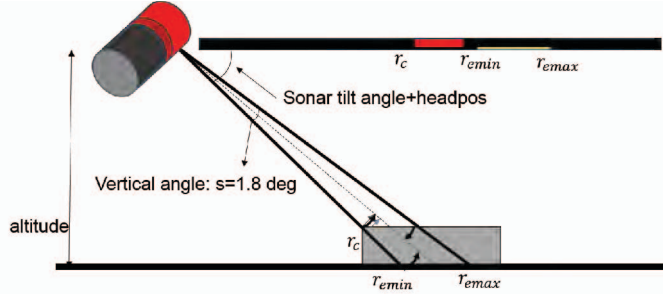


Fig. 2. Geometry of MSPS for Point cloud generation

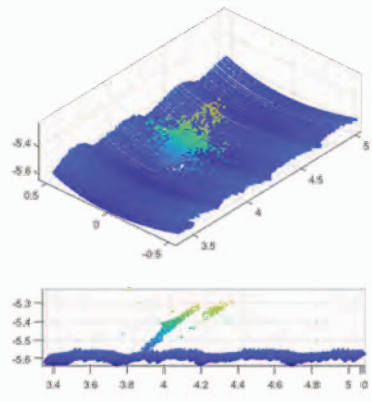


Fig. 3. Generated point cloud by using Cho's method and undesired slope

### III. METHOD

We proposed a method for seabed 3D mapping by using two different types of sonars: ALMS and MSPS. The used sonars are mounted rotated 90 degrees with respect to the each view angle thus they have different viewpoint (Fig. 4). The ALMS obtains horizontal projected image, and the MSPS scans vertical profile of the front area of the sonars. The two sonars are mounted on AUV. When the AUV moves forwardly, then 3D point cloud can be generated [1]. The point generated from two sonars have errors because there is time gap of the data taken from the sonars. To correct the error, a scan matching algorithm is needed. The iterative closest point(ICP) algorithm is both easy to implement and widely used, but it requires many computations. The NDT[2] is more compact

and can save computational load. We adopted NDT algorithm to merge the data set from two sonars

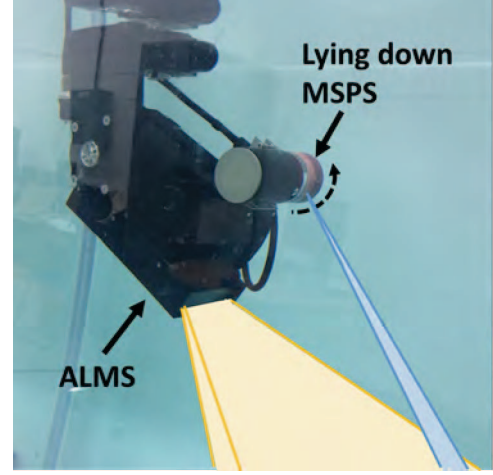


Fig. 4. Assembled ALMS and rotated MSIS

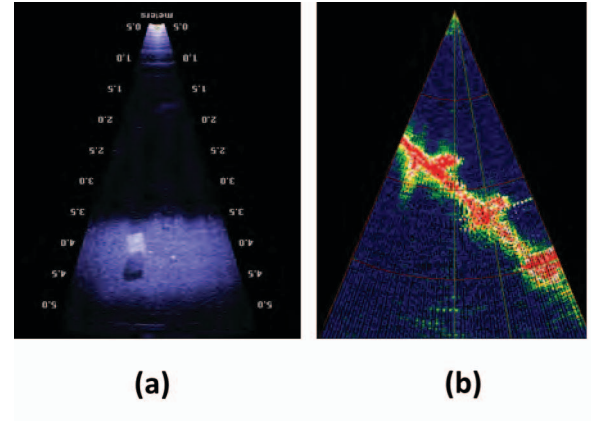


Fig. 5. Example of obtained data from (a) ALMS and (b) MSIS.

#### A. 3D point cloud generation

Wide angle sensors such as sonars, are difficult to measure accurate range because the acoustic waves propagate wide. Therefore, there need some special technique to extract points from sonar data. Cho et al. proposed the 3D point cloud generation method using ALMS [1]. The algorithm for 3D point cloud generation in [1] can be summarized in Algorithm 1, where  $I(x, t)$  is the sonar data, and  $X_r$ ,  $Y_r$ ,  $Z_r$ , and  $H_r$  are AUV position.  $t$  and  $s$  are tilt angle and vertical aov of sonar, and  $T(\cdot)$  transforms real range to corresponding pixel number on the sonar image.  $r_{min}$  and  $r_{max}$  are the minimum and maximum range that the acoustic beam actually can reach on seabed considering vertical angle of beam of sonar.  $r_c$  is the range to the top edge of the object

from sonar, which derives height information of object (Eq. 1).

$$Height = H_r - \frac{r_c}{\cos(0.5s) \sin(t + 0.5s)} \quad (1)$$

---

**Algorithm 1** 3D Point cloud generation method

---

```

function PC_GEN( $I(x, y), \{X_r, Y_r, Z_r, H_r, \phi, \theta, \psi\}$ )
   $r_{emin} \leftarrow \frac{H_r}{\sin(t+0.5s)}$ 
   $r_{emax} \leftarrow \frac{H_r}{\sin(t-0.5s)}$ 
  Transform  $\bar{r}_{emin} = T(r_{emin}), \bar{r}_{emax} = T(r_{emax})$ 
  for all rows  $x_i \in I$  do
    set  $x_i \in S(x, y)$  that  $x_i \leq \bar{r}_{emin}$ 
    set  $x_i \in E(x, y)$  that  $x_i > \bar{r}_{emin}$  and  $x_i \leq \bar{r}_{emax}$ 
  end for
  for all row  $x_i \in S$  do
     $(x, y) = DifferenceFiltering(S(x_i, y))$ 
     $i_{max} = \max((x, y))$ 
    if  $i_{max} > threshold$  then
       $\bar{r}_c \leftarrow i_{max}$ 
    else  $\bar{r}_c \leftarrow \bar{r}_{emax}$ 
    end if
  end for
   $r_c = T^{-1}(\bar{r}_c)$ 
   $\{X, Y, Z\} = \{X_r, Y_r, Z_r\} + r_c \cdot Transform(\phi, \theta, \psi)$ 
return  $\{X, Y, Z\}$ 
end function

```

---

### B. Registration and Mapping

To register this two information into 3D spatial map, we used NDT algorithm [7][8]. The NDT is a grid (or a voxel in 3D) based map representation, which combines the advantages of NDT maps (compactness) and Occupancy maps (robustness). NDT had been proposed by Biber and Straer in [2], and was expanded to 3D by Magnusson [8]. The NDT is the method for compactly representing observed scan data as a set of Gaussian probability distribution. Scan data in each grid is described by the mean and covariance matrix, thus it can save the memory and computing load.

The NDT representation expresses space as grid cell, and a measured data given as points in the global reference frame is added into the grid cell of the map. The points contained in each grid are accumulated and are calculated for the parameters of a normal distribution, which represents the grid cell instead of each point. Given that the reference and the current scan are  $Y = \{y_1, \dots, y_m\}$  and  $X = \{x_1, \dots, x_n\}$ , respectively, then the parameters in grid cell  $Y_n$  can be calculated as,

$$\mu_n = \frac{1}{n_p} \sum_{i: y_i \in Y_n} y_i \quad (2)$$

$$\Sigma_n = \frac{1}{n_p - 1} \sum_{i: y_i \in Y_n} (y_i - \mu_n)(y_i - \mu_n)^T, \quad (3)$$

where  $n_p$  is the number of point in each grid cell. The likelihood between grids and a point in current scan is calculated as sum of normal distribution density function [9]:

$$p(x) = \sum_{i=1}^N c_i \exp\left(-\frac{(x - \mu_n)^T \Sigma^{-1} (x - \mu_n)}{2}\right) \quad (4)$$

To implement the data fusion of sonars for AUV application, several modification was presented. The AUV to be implemented this algorithm is a hovering type AUV, and was designed to have structural stability in roll and pitch by locating the center of buoyance and the center of gravity far from each other as shown in Fig.6. In addition, the AUV moves slowly, thus roll and pitch motion is almost zero. Therefore, we neglected the roll and pitch motion, and the transformation parameter can be simplified as:  $p = [t_x, t_y, t_z, \theta_z]$ , and the NDT algorithm is modeled as 4-DOF. The spatial transformation  $T: X_n \rightarrow X'_n$  between reference and current scan data are given by:

$$T: \begin{pmatrix} x' \\ y' \\ z' \end{pmatrix} = \begin{pmatrix} \cos \theta_z & -\sin \theta_z & 0 \\ \sin \theta_z & \cos \theta_z & 0 \\ 0 & 0 & 1 \end{pmatrix} \begin{pmatrix} x \\ y \\ z \end{pmatrix} + \begin{pmatrix} t_x \\ t_y \\ t_z \end{pmatrix} \quad (5)$$

If only closest grid is considered, the likelihood function of a

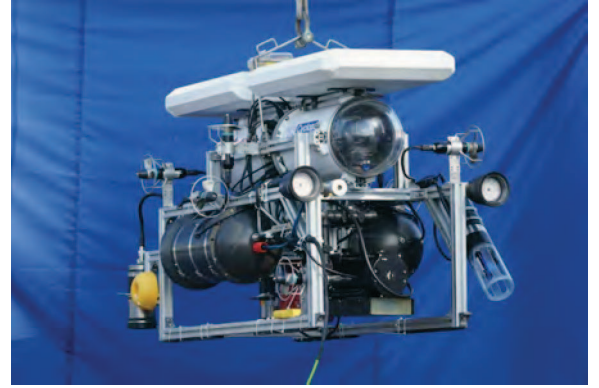


Fig. 6. The hovering type AUV Cyclops

transformed point to the closest grid cell is expressed as:

$$p(x'_n | \mu_c, \Sigma_c) = c_2 \exp\left(-\frac{(x'_n - \mu_c)^T \Sigma_c^{-1} (x'_n - \mu_c)}{2}\right). \quad (6)$$

The score function and cost function to be minimized are derived as:

$$score(p, x_n, c) = c_3 \exp\left(-\frac{q^T \Sigma_c^{-1} q}{2}\right), \quad (7)$$

$$cost(p) = -\sum_{i=1}^n score(p, x_n, c), \quad (8)$$

where  $c$  is closest grid cell, and  $q = (x'_n - \mu_c)$ . By minimizing the cost function, the transformation parameters can be estimated. To solve the optimization problem, we used Newton's method.

The Newton's method solves the following equation:

$$H\Delta p = -g, \quad (9)$$

where  $H$  and  $g$  are hessian matrix and gradient of the score function.  $\Delta p$  is an increment of  $p$ , thus the transformation parameter is updated as follows:

$$p \leftarrow p + \Delta p. \quad (10)$$

The entries of the gradient of the score function is derived as:

$$g_i = -\frac{\partial f}{\partial p_i} = q^T \Sigma^{-1} \frac{\partial q}{\partial p_i} \exp\left(\frac{q^T \Sigma^{-1} q}{2}\right), \quad (11)$$

where  $\frac{\partial q}{\partial p_i}$  composes Jacobian matrix as:

$$J = \begin{pmatrix} 1 & 0 & 0 & -x \sin \theta_z - y \cos \theta_z \\ 0 & 1 & 0 & x \cos \theta_z - y \sin \theta_z \\ 0 & 0 & 1 & 0 \end{pmatrix}. \quad (12)$$

The entries of Hessian of the score function are given by:

$$H_{ij} = \frac{\partial^2 f}{\partial p_i \partial p_j} = ((-q^T \Sigma^{-1} \frac{\partial q}{\partial p_i})(-q^T \Sigma^{-1} \frac{\partial q}{\partial p_j}) \quad (13)$$

$$+ (-q^T \Sigma^{-1} \frac{\partial^2 q}{\partial p_i \partial p_j}) \quad (14)$$

$$+ (-\frac{\partial q^T}{\partial p_j} \Sigma^{-1} \frac{\partial q}{\partial p_i})(-\exp(\frac{q^T \Sigma^{-1} q}{2})), \quad (15)$$

where the second derivative of  $q$  is:

$$\frac{\partial^2 q}{\partial p_i \partial p_j} = \begin{pmatrix} \vec{0} & \vec{0} & \vec{0} & \vec{0} \\ \vec{0} & \vec{0} & \vec{0} & \vec{0} \\ \vec{0} & \vec{0} & \vec{0} & \vec{0} \\ \vec{0} & \vec{0} & \vec{0} & \vec{a} \end{pmatrix}, \quad (16)$$

where

$$\vec{a} = \begin{pmatrix} -x \cos \theta_z + y \sin \theta_z \\ -x \sin \theta_z - y \cos \theta_z \\ 0 \end{pmatrix}. \quad (17)$$

To avoid singular matrix of the covariance and Hessian matrix, grid cells is considered as occupied when they have 4 more points. In addition, when matrix is singular, we adjust the smallest eigenvalue of the matrix about 100 times.

#### IV. EXPERIMENT AND RESULTS

##### A. Experimental setup

The proposed method was tested by indoor tank test using AUV. The AUV was developed at Harzadous and Extreme Robotics Laboratory at the Pohang University of Science and Technology (POSTECH) [11]. The experimental setup was as shown in Fig. 7 and 8. 3 objects were located on the bottom of the water tank: a concrete block, an aluminum cylinder, and a plastic basket. In the test the AUV kept its altitude and heading constant, and moved slowly along the pre-determined waypoints. ALMS acquired 512 by 96 acoustic images with the vertical angle of view of 14 degrees, and MSIS scans 500 by 1 echos with vertical angle of view of 1.8 degrees. Both

sonars updated their data with 0.1-Hz frequency. The tilt angle of sonar was 45.19 degrees.

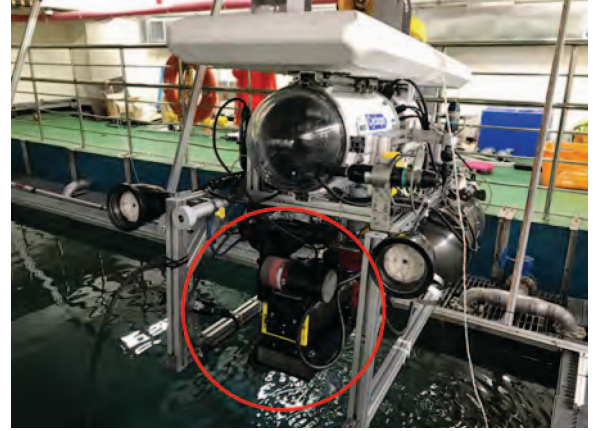


Fig. 7. Two sonars equipped AUV Cyclops

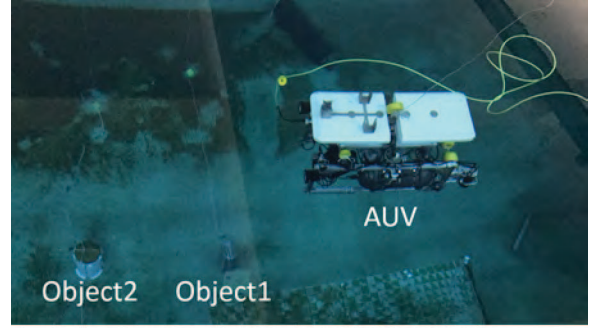


Fig. 8. Experimental setup

##### B. Results

The results of 3D point cloud without NDT was presented in Fig. 9. The AUV collected 459168 points from ALMS and 4783 points from MSPS, respectively. Since the MSPS can scan longer distance than ALMS, the MSPS acquired data in short time with less drift error. As shown in Fig. 9, the two point clouds were misaligned due to drift error and position control error of AUV. The results of 3D point cloud with NDT was presented in Fig. 10. After applying NDT, the misaligned error was eliminated, and we obtained more consistent point cloud.

#### V. CONCLUSION

We presented and implemented 3D point cloud mapping by using NDT algorithm to combine data set obtained from two different types of sonars. Considering the motion characteristic of AUV, we derived 4-DOF NDT algorithm and tested it in indoor water tank. As a result, we obtained consistent 3D point cloud map. Most of underwater map generation method performed by offline post processing. Since NDT algorithm is very compact and easy to use, it can be used for online map building. As a future work, we will develop efficient



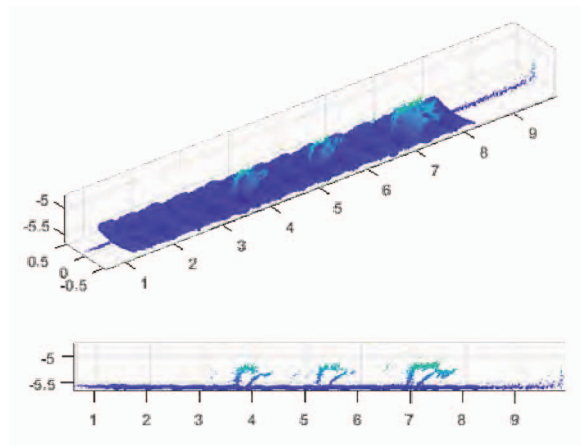


Fig. 9. Point cloud representation without scan matching

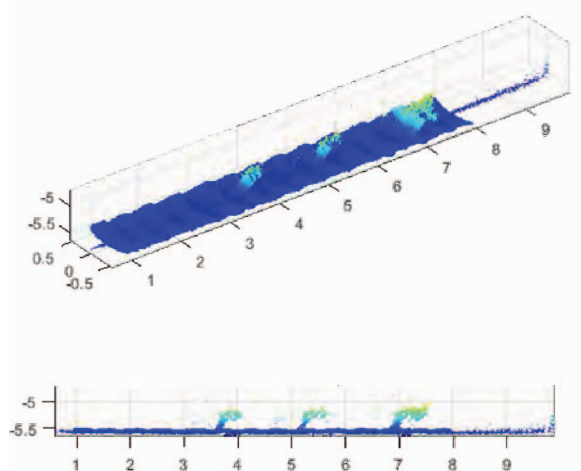


Fig. 10. Point cloud representation after scan matching

segmentation method to separate seabed and object, then will apply this algorithm to the object part, which can improve the speed of scan matching. Finally, we will expand to underwater SLAM for self-localizing long-range AUVs.

#### ACKNOWLEDGMENT

This research was supported by the MSIT(Ministry of Science and ICT), Korea, under the ICT Consilience Creative program(IITP-2017-R0346-16-1007) supervised by the IITP(Institute for Information & communications Technology Promotion), and the National Research Foundation of Korea(NRF) grant funded by the Korea government(MSIT) (No. 2017R1A5A1014883). In addition, this research was a part of the project titled Gyeongbuk Sea Grant, funded by the Ministry of Oceans and Fisheries, Korea.

#### REFERENCES

- [1] Cho, Hyeonwoo, Byeongjin Kim, and Son-Cheol Yu. "AUV-Based Underwater 3-D Point Cloud Generation Us-

- ing Acoustic Lens-Based Multibeam Sonar." *IEEE Journal of Oceanic Engineering*, 2017.
- [2] Biber, Peter, and Wolfgang Straer. "The normal distributions transform: A new approach to laser scan matching." *Intelligent Robots and Systems, 2003.(IROS 2003). Proceedings. 2003 IEEE/RSJ International Conference on*. Vol. 3. IEEE, 2003.
- [3] Langer, Dirk, and Martial Hebert. "Building qualitative elevation maps from side scan sonar data for autonomous underwater navigation." *Robotics and Automation, 1991. Proceedings., 1991 IEEE International Conference on*. IEEE, 1991.
- [4] Yu, Son-Cheol. "Development of real-time acoustic image recognition system using by autonomous marine vehicle." *Ocean Engineering* 35.1 (2008): 90-105.
- [5] Cho, Hyeonwoo, et al. "Acoustic beam profile-based rapid underwater object detection for an imaging sonar." *Journal of Marine Science and Technology* 20.1 (2015): 180-197.
- [6] Fairfield, Nathaniel, George Kantor, and David Wettergreen. "RealTime SLAM with Octree Evidence Grids for Exploration in Underwater Tunnels." *Journal of Field Robotics* 24.12 (2007): 03-21.
- [7] Saarinen, Jari P., et al. "3D normal distributions transform occupancy maps: An efficient representation for mapping in dynamic environments." *The International Journal of Robotics Research* 32.14 (2013): 1627-1644.
- [8] Magnusson, Martin. *The three-dimensional normal-distributions transform: an efficient representation for registration, surface analysis, and loop detection*. Diss. rebro universitet, 2009.
- [9] Kim J. 3-D Scan Registration Using Normal Distributions Transform with Supervoxel Segmentation. Diss. Seoul National University, 2015.
- [10] Einhorn, Erik, and Horst-Michael Gross. "Generic NDT mapping in dynamic environments and its application for lifelong SLAM." *Robotics and Autonomous Systems* 69 (2015): 28-39.
- [11] Pyo, Juhyun, et al. "Development of hovering type AUV Cyclops and its performance evaluation using image mosaicing." *Ocean Engineering* 109 (2015): 517-530.